Journal of Hazardous Materials 457 (2023) 131817

Contents lists available at ScienceDirect

Journal of Hazardous Materials

journal homepage: www.elsevier.com/locate/jhazmat

Super-oxidized "activated graphene" as 3D analogue of defect graphene oxide: Oxidation degree vs U(VI) sorption

Nicolas Boulanger [a], Gui Li [a], Tamuna Bakhiia [b], Konstantin I. Maslakov [b], Anna Yu. Romanchuk [b], Stepan N. Kalmykov [b,*], Alexandr V. Talyzin [a,*]

[a] Department of Physics, Umeå University, S-90187 Umeå, Sweden
[b] Department of Chemistry, Lomonosov Moscow State University, Leninskie Gory, Moscow 119991, Russia

HIGHLIGHTS

- High surface area carbon materials can be oxidized to the same degree of standard graphene oxide.
- The sorption of U(VI) increases proportionally to oxidation degree of material.
- Super-oxidized "activated graphene" shows huge increase of U(VI) sorption up to 5400 μmol/g.
- Sorption of U(VI) can be further increased by 2–3 times using general trend provided in our study.

GRAPHICAL ABSTRACT

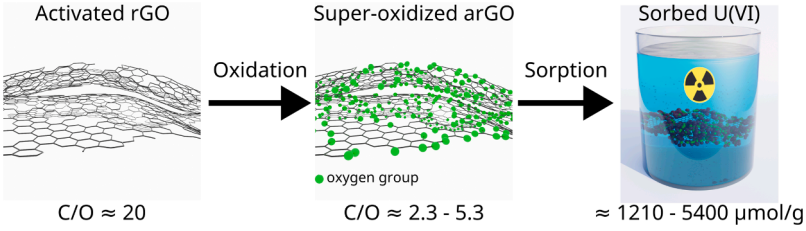

ARTICLE INFO

Editor: Sungjun Bae

Keywords:
Absorbent
Uranium
Porous carbon
Carbon material
Chemical modification

ABSTRACT

Porous carbons are not favorable for sorption of heavy metals and radionuclides due to absence of suitable binding sites. In this study we explored the limits for surface oxidation of "activated graphene" (AG), porous carbon material with the specific surface area of ~2700 m^2/g produced by activation of reduced graphene oxide (GO). Set of "Super-Oxidized Activated Graphene" (SOAG) materials with high abundance of carboxylic groups on the surface were produced using "soft" oxidation. High degree of oxidation comparable to standard GO (C/O=2.3) was achieved while keeping 3D porous structure with specific surface area of ~700–800 m^2/. The decrease in surface area is related to the oxidation-driven collapse of mesopores while micropores showed higher stability. The increase in the oxidation degree of SOAG is found to result in progressively higher sorption of U (VI), mostly related to the increase in abundance of carboxylic groups. The SOAG demonstrated extraordinarily high sorption of U(VI) with the maximal capacity up to 5400 μmol/g, that is 8.4 – fold increase compared to non-oxidized precursor AG, ~50 –fold increase compared to standard graphene oxide and twice higher than extremely defect-rich graphene oxide. The trends revealed here show a way to further increase sorption if similar oxidation degree is achieved with smaller sacrifice of surface area.

1. Introduction

New sorbent materials are required to remove various kinds of contaminants from natural waters and industrial aqueous waste solutions. Clay minerals, e.g. bentonites, have been the main industrial sorbent material used for radionuclide waste disposal over past decades. These materials swell in water [1] thus providing access to the surface of individual 2D clay flakes and demonstrating high ion exchange capacity

* Corresponding authors.
E-mail addresses: stepan@radio.chem.msu.ru (S.N. Kalmykov), alexandr.talyzin@umu.se (A.V. Talyzin).

https://doi.org/10.1016/j.jhazmat.2023.131817
Received 24 April 2023; Received in revised form 5 June 2023; Accepted 7 June 2023
Available online 10 June 2023

for sorption of various ions, including actinide ions. Graphene oxides (GO) are also materials with strong swelling in water and high ion exchange capacity, sometimes named as "organic clay".[2–5] However, GO only relatively recently attracted attention for sorption of radionuclides demonstrating effectiveness far exceeding that of bentonites or activated carbons [6]. Remarkably, the theoretical specific surface area of GO is much higher (~2400 m^2/g) than that of bentonites (~800 m^2/g [7]) but still lower than the specific surface area of some porous carbons, e.g. ~3000 m^2/g for some activated carbons [8] and "activated graphene" (AG) [9–11]. However, the BET Specific Surface Area (SSA) of bulk powder GO is negligibly small due to the structure not allowing nitrogen to access the inter-layer space. Therefore, GO needs to be dispersed into true 2D sheets in suitable polar solvent to serve as a sorbent. The experimental surface area of GO measured in aqueous dispersions by the sorption of various molecules is much smaller than the theoretical value of 700–800 m^2/g [12,13]. Preparation of dispersions and removal of GO from solutions are technological steps, which complicate practical applications of these materials. On the other hand, high surface area porous carbons are hydrophobic and not good for removal of radionuclides due to the absence of suitable binding sites.

Therefore, carbon materials with high specific surface area need to be chemically modified for removal of cationic radionuclides and heavy metals from aqueous solutions. For example graphene is hydrophobic, but its oxidized form, GO is hydrophilic and shows much higher sorption capacity for removal of cation contaminations.[6,14] Our recent work also established a direct correlation between the defect state of GO and amount of sorbed radionuclides [15]. We demonstrated that extremely defected graphene oxide (dGO) provides a 15-fold increase in sorption capacity of U(VI) compared to standard GO.[16] However, dGO is rather exotic material with unlikely chances for scaled up production. Moreover, attempts to produce even stronger oxidized dGO failed due to breaks up of GO sheets on rather small nm sized particles, which were extremely challenging to remove from solutions by filtration or centrifuging. It is also unlikely that further increase of U(VI) sorption can be achieved by chemical functionalization of GO.

Therefore, we suggested a new concept to create materials very similar to GO in terms of surface oxidation, but with a stable 3D structure and extremely high specific surface area. Many surface oxidation methods have been previously tested for carbon nanotubes,[17] activated carbons[18] and natural carbon materials [19]. However, only very few of these materials have been tested in the sorption of radionuclides. Moreover, oxidation often results in a significant loss of the specific surface area of the carbon material. The specific surface area of oxidized carbon materials tested for sorption applications sometimes is rather small, e.g. < 20 m^2/g for carbons produced by permanganate oxidation [19].

After testing several surface oxidation methods, we were able to convert hydrophobic "activated graphene" into hydrophilic material with main properties similar to GO but rigid 3D structure.[20] The high sorption capacity of dGO and Super Oxidized Activated Graphene (SOAG) towards radionuclides is explained by the high abundance of defects and oxygen functional groups attached to these defects. Modelling of sorption mechanism showed that carboxylic groups are most likely responsible for the high U(VI) sorption of these materials. The preferential interaction of metal cations with carboxylic groups is also in agreement with independent studies [21,22].

It can be assumed that carbon materials optimized for sorption of radionuclides should be well oxidized and provide as high surface area as possible. The only SOAG sample so far tested for U(VI) sorption in our earlier study showed a relatively small oxidation degree (C/O=3.3) and specific surface area of about ~800 m^2/g. [20] The sorption of U(VI) measured for this material was high but not superior to dGO.[16] It seem to be extremely important to establish clear trends in a degree and type of oxygen functionalization in order to increase of sorption capacity of porous carbon materials over the capacity of chemically modified graphene oxides.

In this study we produced surface oxidized activated graphene with different oxidation degree exploring the limits of AG stability against oxidation-induced pore collapse and decrease of surface area. It is demonstrated that prolonged oxidation saturates at C/O value of ~2.3–2.4 and SSA of ~700–800 m^2/g. Oxidation results in the significant increase in the maximal U(VI) sorption. An extremely high sorption capacity of ~5400 μmol/g (at pH 5.1) was achieved for material with the highest oxidation degree. That is despite the significant oxidation-induced decrease in the specific surface area due to collapse of mesopores. Our results provide important trends for further increase of U(VI) sorption by carbon materials emphasizing the superior importance of high oxidation degree. The trends revealed in our study are likely to lead to 2–3-fold higher sorption capacity of SOAG if the same oxidation degree can be achieved without sacrificing surface area.

2. Experimental

2.1. Materials

Graphite oxide powder was purchased from Abalonyx (Norway). Activated carbon (YP-80 F) was provided by Kuraray Co., Ltd (Japan).

2.2. Synthesis and characterization of SOAG

Activated reduced graphene oxide (AG or "activated graphene") was synthesized using the procedure optimized in our earlier studies for maximal specific surface area.[9,10] The procedure includes explosive exfoliation of graphite oxide to produce rGO with high specific surface area and KOH activation of rGO to prepare AG. Graphite oxide was placed into a large volume aluminum cylinder and explosively exfoliated by rapid insertion of sample into a hot furnace at ~230 °C. The sample was removed from the furnace after about 8 min.

The exfoliated rGO material was then mixed with potassium hydroxide in a 1–8 wt ratio in a 70% vol. solution of ethanol in water and left stirring overnight. The material was dried in a vacuum oven heated at 80 °C overnight before being placed in an alumina boat and loaded in a tube furnace under an argon flow. The tube was then heated to 200 °C for 1 h in order to remove all water, subjected to temperature ramping up to 850 °C, annealed at that temperature for 3 h and cooled down inside the furnace. The activated material was then placed in a 10% acetic acid solution and stirred overnight before being rinsed with DI water in a vacuum filtration setup and left to dry in a vacuum oven. Activated carbon YP-80 F by Kuraray Co., Ltd. with BET SSA of ~2580 m^2/g was used in reference oxidation test.

The BET SSA, cumulative SSA and pore size distribution of materials were determined using analysis of nitrogen sorption isotherms. The AG was amorphous according to the XRD analysis and showed typical for this kind of material Raman spectra dominated by the G- and D-modes.

The AG was then placed in the saturated solution of ammonium persulfate in water (~200 mg of dry material for 20 mL of solution) and the dispersion was stirred continuously at room temperature for the desired oxidation time. The dispersion was finally rinsed using vacuum filtration and DI water before being dried in a vacuum oven at room temperature.

XPS spectra were recorded using Kratos Axis Ultra electron spectrometer equipped with a delay line detector. A monochromatic Al Kα source operated at 150 W, a hybrid lens system with a magnetic lens, providing an analysis area of 0.3 × 0.7 mm, and a charge neutralizer were used for the measurements. The binding energy scale was adjusted with respect to the C1s line of aliphatic carbon, set at 285.0 eV. All spectra were processed with the Kratos software. TGA data were recorded using a Mettler Toledo TGA/DSC1 STARe System. Experiments were performed from room temperature up to 700 °C at a heating rate of 3 K min^{-1} under nitrogen or air flow (40 mL min^{-1}). A Panalytical X'pert diffractometer was used to record XRD patterns in reflection mode with CuKα radiation. Raman spectra were recorded using a

Renishaw Invia Raman spectrometer equipped with 514 nm laser. Fourier transform infrared (FTIR) spectra were recorded from powder samples using a Bruker IFS 66 v spectrometer under vacuum conditions. The nitrogen sorption isotherms were measured at liquid nitrogen temperature using an Autosorb iQ XR surface area & pore size analyzer by Quantachrome equipped with a turbo pump. The relative pressure interval P/P_0 for the BET plot was selected using a procedure optimized for microporous materials. The procedure takes into account Rouquerol parameters provided as a part of standard Quantachrome ASiQWin software package.[23] As verified by tests, this procedure provides identical values as BETSI software.[24] The slit-pore QSDFT equilibrium model was applied to evaluate cumulative surface area, pore volume and pore size distribution.

The pore volume available for the sorption of liquid water was determined using the DSC method by comparing the enthalpy of pure water melting and enthalpy of melting of the same amount of water with known amount of added porous material. It is known that the freezing and melting of water confinement do not occur in pores smaller than ~2 nm [25]. This effect is routinely used for evaluation of the solvent amount sorbed by porous materials at the temperature of solvent (water) melting T_m [26]. The non-freezable water does not contribute to the measured melting enthalpy. Therefore, the DSC peak due to the melting of bulk water will be smaller than expected if part of water is adsorbed by nanoporous material. The decrease in melting enthalpy measured using DSC allows calculation of the amount of solvent sorbed by the material in pores smaller than ~2 nm. The quantitative measurements were performed using a STARe system DSC 3 by Mettler Toledo under flow of nitrogen.

2.3. U(VI) sorption experiments

All sorption experiments were carried out in plastic vials with minimal retention by walls. A mixture of $^{232,233}U$ and natural uranium was utilized to create a wide range of concentration for measuring sorption isotherms. Aliquots of uranium (uranyl nitrate) were added to a 0 – 0.1 g/L suspension of SOAG materials in 0.1 M $NaClO_4$. The pH value was measured using a combined glass pH electrode (InLab Expert Pro, Mettler Toledo) with an ionomer (SevenEasy pH S20-K, Mettler Toledo) and was adjusted to 5.10 ± 0.05 via the addition of small amounts of diluted $HClO_4$ or NaOH. After several days of equilibration pH was checked again and corrected to 5.10 if needed. Then pH stabilized at the required value the aliquot of the suspensions was centrifuged at 40,000 g for 20 min (Allegra 64 R, Beckman Coulter) to separate the solid phase from the solution. The sorption capacity was calculated as a difference between the initial activity of the radionuclides and the activity measured in the solution after centrifugation. The activity of radionuclides was measured by liquid-scintillation spectroscopy (Quantulus-1220, Perkin Elmer).

3. Results and discussion

3.1. Synthesis and characterization of surface oxidized activated graphene

The samples with progressively stronger oxidation were prepared using a single batch of AG with SSA of 2677 m^2/g and C/O= 19.6. The characterization of precursor AG is summarized in SI file, more details can be also found in our earlier studies[10,20]. Shortly, AG is nearly completely amorphous material according to XRD showing only some diffuse scattering in the low angle region (Fig. S1 in SI file). AG shows a pore size distribution with micro- and mesopores. The pore diameter is mostly below 4 nm as revealed by the analysis of nitrogen sorption isotherms (Fig. 1, a and b). Porous nature of this material was also confirmed by electron microscopy imaging (Fig. 2, see also Fig. S2 in SI file). A similar batch was also earlier characterized using high resolution STEM, showing directly presence of nm-sized pores [20].

The AG powder was subjected to ammonium persulfate oxidation treatment for different periods of time (1–14 days). The oxidation degree was controlled by XPS. A decrease in C/O ratio from 19.6 for precursor AG down to 2.3 was observed for the sample oxidized for 14 days. Therefore, the prolonged oxidation of AG produced the material with the oxidation degree similar to that in standard graphite oxide (C/O~2.4–2.6 [3,27]) (Table 1).

It is interesting to note that AG seem to show the increased stability of structure during oxidation compared to standard activated carbons. Activated carbon could be considered as an inexpensive precursor alternative to AG for producing surface oxidized carbon materials. The same oxidation treatment (14 days in ammonium persulfate) was applied to the sample of standard commercial activated carbon with initial SSA of ~ 2500 m^2/g. However, oxidation resulted in complete collapse of porous structure of activated carbon with BET SSA dropping down to 37 m^2/g (Fig. S6). Therefore, no further experiments were performed here to study oxidation of activated carbon.

In contrast to graphite/graphene oxides, SOAG maintain porous 3D structure with relatively high SSA, (~690 m^2/g for the sample with C/O=2.3), as determined using analysis of nitrogen sorption isotherms (Fig. 1).

The strong oxidation of AG decreases the specific surface area due to a partial collapse of the porous structure. The precursor AG shows pore size distribution which includes significant fraction of pores with

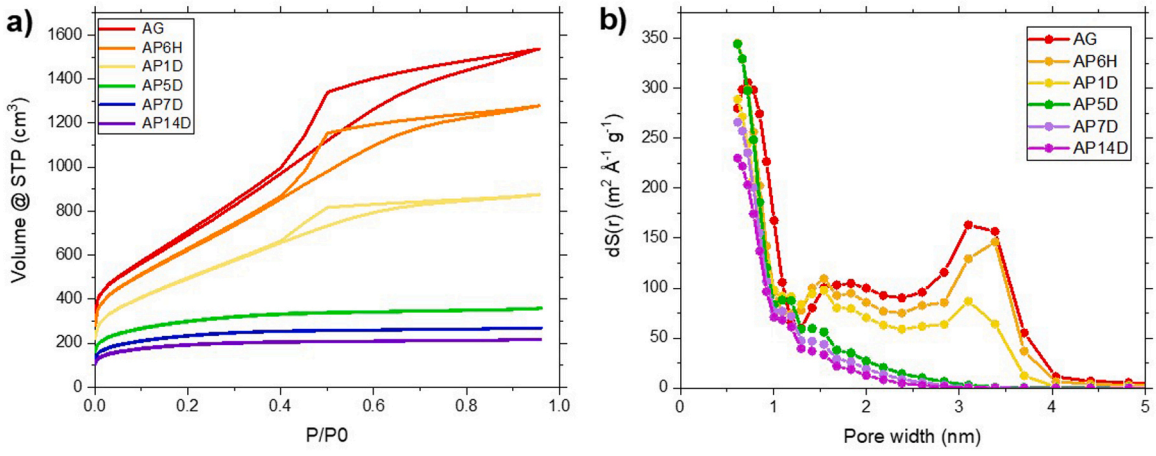

Fig. 1. a) Nitrogen sorption isotherms and b) pore size distribution of SOAG samples (QSDFT model) produced using different oxidation time (6 h – 14 days). Prolonged oxidation resulted in a collapses of 2–4 nm pores while smaller pores mostly preserved.

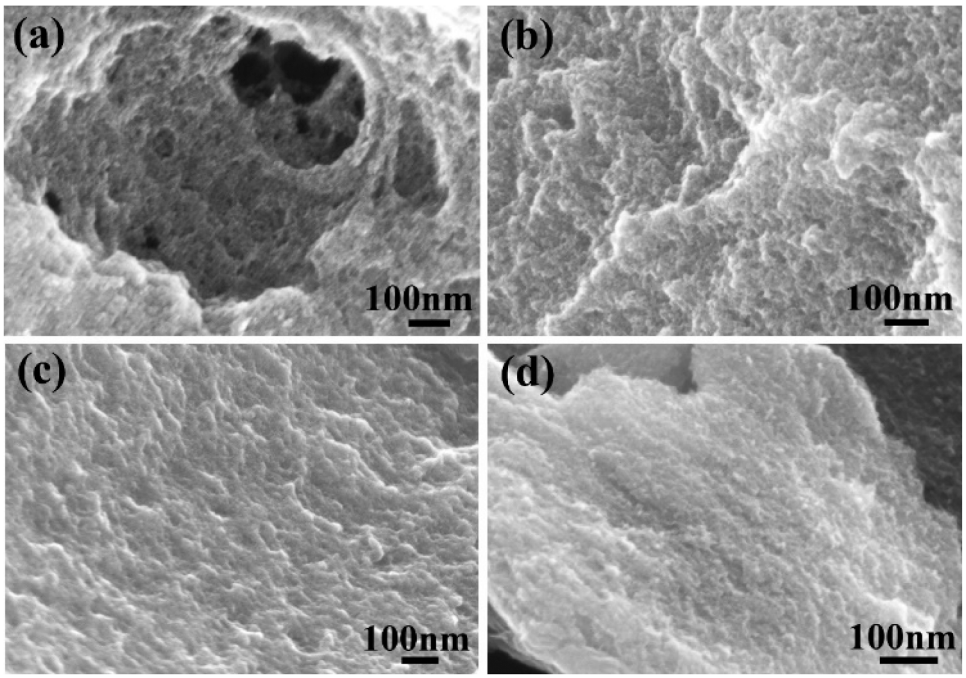

Fig. 2. SEM images of AG before and after oxidation. SEM images of precursor AG (a) and AG samples oxidized for 2 days (b), 7 days (c) and 14 days (d).

Table 1
Main properties of AG samples oxidized using ammonium persulfate for different periods of time. The columns from left to right: name of sample, duration of oxidative treatment, BET SSA, Cumulative SSA by QSDFT method, cumulative pore volume (QSDFT), C/O ratio calculated using analysis of XPS spectra, oxygen content according to COx formula, sorption of water determined using the DSC method and sorption of U(VI) determined by the batch method.

Name	Oxidation time	BET SSA (m^2/g)	Cumul. SSA (m^2/g)	Cumul. volume (cm^3/g)	C/O	Formula	Liquid water sorption (mg H_2O/ mg SOAG)	Sorption capacity at pH 5.1 (μmol/g)
AG	Precursor	2677	2191	2.27	19.6	$CO_{0.05}$	3.25	640 ± 80
AP6H	6 hrs	2348	1984	1.88	5.3	$CO_{0.19}$	2.21	1210 ± 60
AP1D	1 day	1819	1535	1.28	3.8	$CO_{0.26}$	1.92	2930 ± 250
AP3D	3 days	1602	1389	0.9	n/a	n/a	1.18	3300 ± 100
AP5D	5 days	1069	1012	0.51	2.7	$CO_{0.38}$	0.81	3560 ± 70
AP7D	7 days	838	790	0.39	2.4	$CO_{0.42}$	0.66	4000 ± 100
AP14D	14 days	693	664	0.31	2.3	$CO_{0.43}$	0.66	5400 ± 300

~3–4 nm width. Strongly oxidized samples (treated for 5–15 days) preserve only smallest pores (< 1 nm), whereas larger pores disappear (Fig. 1b). The specific surface area decrease from 2677 m^2/g in precursor AG down to ~700–800 m^2/g in the most strongly oxidized SOAG samples could be explained partly by the addition of more heavy oxygen (up to ~20% decrease of SSA). Addition of functional groups to inner pore walls could also decrease the pore size and, therefore, the SSA. It is reasonable to estimate the decrease in pore size due to functionalization of carbon pore with oxygen groups to be at least on the level of ~0.35 nm, similar to the difference in interlayer distances in graphene and graphene oxide (0.34 and ~0.7 nm respectively). However, collapse of larger pores (3–4 nm) is the main reason for the decreased specific surface area of strongly oxidized samples according to the change in pore size distribution, Fig. 1b. This conclusion is confirmed by the cumulative surface area plots of SOAG samples as a function of pore size (Fig. S5 in SI file). Partial pore collapse is also evident from the decrease in total pore volume estimated from N_2 sorption isotherms and the measurements of liquid water sorption by DSC method (Table 1). The sorption of water decreased approximately 5-fold reflecting the change in the pore volume and collapse of the largest pores.

The combination of high oxidation degree, microporous structure and relatively high surface area are unique properties of SOAG materials. Remarkably, the type of oxidation of SOAG is rather similar to strongly defected graphene oxides as confirmed by XPS, FTIR spectra and TGA tests. The TGA trace of the sample with the highest oxidation time (AP14D sample, see SI file) shows a weight loss of about 56% in the temperature region up to 700 °C. The main weight loss steps found in this curve are related to water evaporation around 100 °C and thermal deoxygenation (~150–200 °C). The temperature intervals are qualitatively similar to those found in typical TGA curves of standard Hummers GO and dGO (see Fig. S4). The amount of water released during the heating in TGA experiment and the weight loss due to de-oxygenation steps are increased for SOAG samples with longer oxidation time (see Fig. S3 in SI file).

Strong oxidation converts hydrophobic AG into progressively more hydrophilic SOAG materials as evidenced by higher water desorption in the TGA scans of stronger oxidized sample. The hydrophilic nature of SOAG with high oxidation degree (C/O=3.3) was also demonstrated in our earlier study using dynamic water vapor sorption method. The water sorption isotherms recorded from SOAG are similar to those obtained for GO and very different compared to isotherms recorded from hydrophobic precursor AG [20].

The XPS spectra recorded from the strongly oxidized SOAG samples show a high intensity of the C—O (286.5 eV) and COOH (288.4 eV) components in the C1s spectra (Fig. 3). The relative intensity of all C1s components due to carbons bound to oxygen functional groups clearly

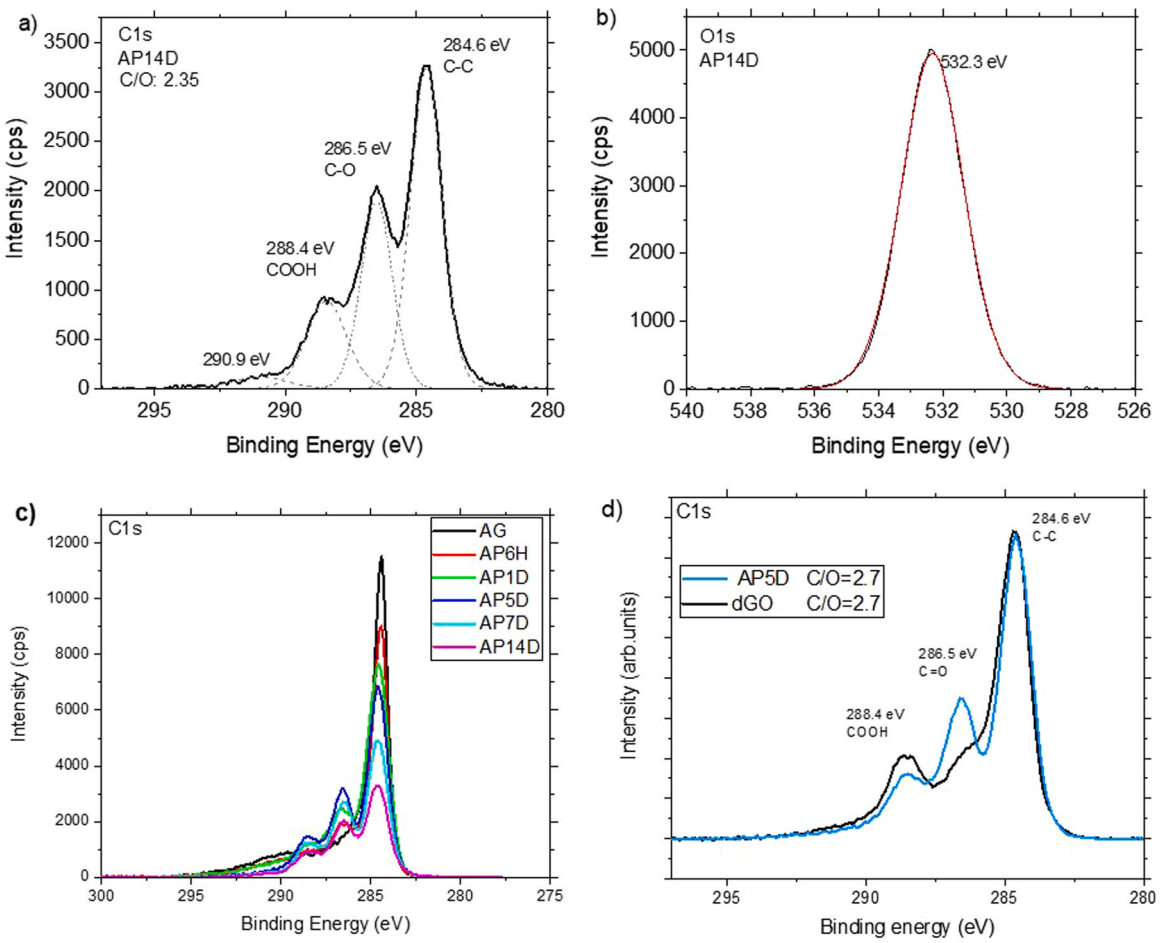

Fig. 3. XPS spectra of oxidized samples. XPS spectra of SOAG produced by oxidation of AG for 14 days (sample with strongest oxidation): a) C1s spectra and b) O1s spectra. XPS spectra recorded from the set of samples oxidized for 6 h to 14 days: c) C1s spectra of samples with progressively longer oxidation time and d) C1s spectra of dGO and AP5D samples with the same oxidation degree (C/O ratio). The spectra were normalized to the intensity of the 284.6 eV component.

increases in the samples oxidized for longer time (Fig. 3c). Notably, not only the overall oxidation degree increases in the samples subjected to longer oxidation, but also the percentages of carbon atoms double bonded with oxygen (carboxyls and carbonyls) Table 2.

It is also interesting to compare the C1s spectra of SOAG samples with the spectra of dGO reported in our earlier studies (Fig. 3d) [16]. The AG sample oxidized for 5 days shows the same C/O ratio as dGO according to the XPS data. The C1s spectra of both materials show strong contributions from the C−O and COOH functional groups but with somewhat different relative intensities. The dGO sample consists of rather small particles (few tens of nm) and shows somewhat higher relative abundance of COOH groups typically found on the edges of flakes and edges of holes in flakes. Nevertheless, the XPS spectra show a remarkable similarity in the type of functionalization for two very different materials with the close oxidation degrees.

The strong oxidation of SOAG is also reflected in the FTIR spectra that demonstrate additional (compared to precursor AG) peaks due to oxygen functional groups (Fig. 4). For example, the relative intensity of the 1712 cm^{-1} peak typically assigned to C═O stretch increases with increasing the oxidation time. The FTIR spectra of SOAG also show rather a broad major feature centered approximately at 1200–1220 cm^{-1} originating most likely from C−O stretch. This feature is typically much less pronounced for standard GO but similarly strong in extremely defect-rich GO reported in our earlier studies.[16]

Overall, SOAG can be considered as an analogue of extremely defect-rich GO with a similar type of oxidation but with the 3D porous structure. Notably, GO needs to be dispersed in suitable solvent (e.g. water) to expose surface for sorption of various ions, while undispersed SOAG has a high surface area thanks to its 3D structure.

Table 2
Relative amount of carbon atoms in C-C and oxygen functional groups according to fitting of C1s XPS spectra (Fig. 3a,c). The reference values calculated with the same fit model for HGO[15] and dGO[16] samples reported in earlier publications. Note that carboxylic groups are not resolved in XPS from carbonyls, the same is for C-O component which includes contributions from hydroxyl and epoxy groups.

Sample	C-C (%)	C-O, C-OH (%)	COOH,C═O (%)
AG	76	21	3
AP6H	71	23	6
AP1D	63	28	9
AP5D	56	29	15
AP7D	53	31	16
AP14D	52	30	18
HGO	38	54	8
dGO 1:1	56	26	18

3.2. U(VI) sorption by progressively stronger oxidized SOAG materials

The main properties of the SOAG samples prepared using different duration of oxidative treatment of AG are summarized in Table 1. Longer treatment produces more oxidized SOAG material but at the cost of lower specific surface area due to collapse of mesopores. This set of samples allowed us to trace the correlations of U(VI) sorption with the specific surface area, oxidation degree and pore volume. Isotherms of U

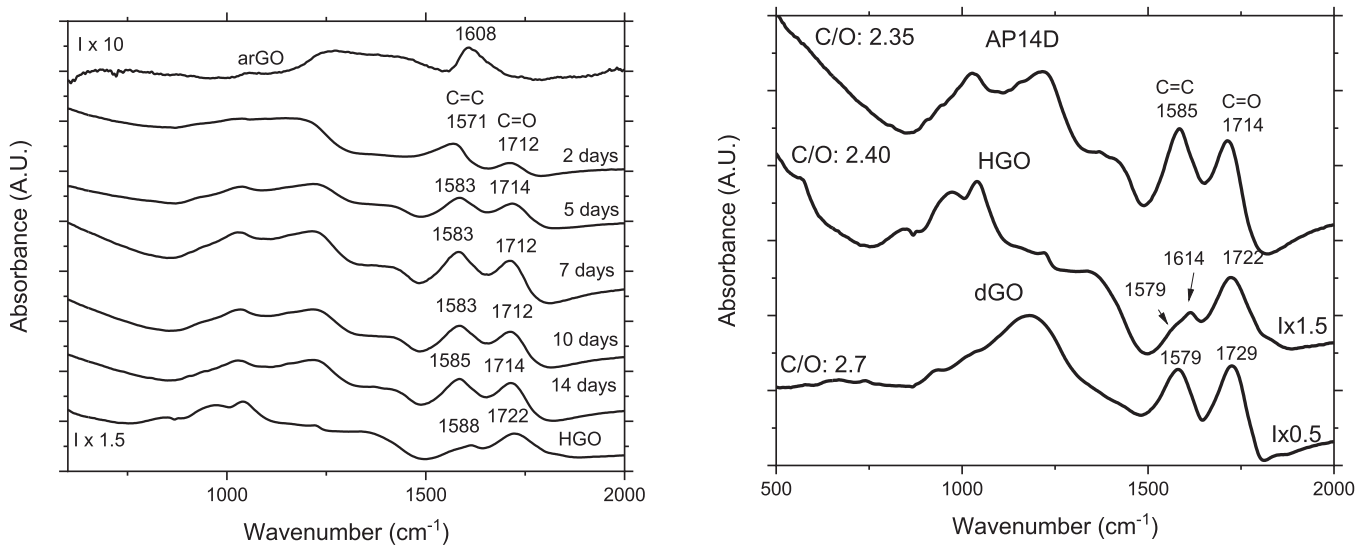

Fig. 4. FTIR spectra of SOAG samples with progressively stronger oxidation. FTIR spectra recorded under vacuum conditions from precursor AG and from samples obtained by oxidation treatment with ammonium persulfate for different times. Spectrum of Hummers GO (HGO) with oxidation degree similar to the most oxidized SOAG is added as a reference.

(VI) sorption were measured at pH 5.1 (Fig. 5). The sorption of U(VI) on the non-oxidized sample (AG) is relatively low. Oxidation treatment gradually increases both the number of oxygen functional groups on the surface of SOAG and U(VI) sorption. The trend observed in the Fig. 5 is very clear: longer oxidation treatment results in higher sorption of uranium. The sorption isotherms were used to determine the maximum sorption capacity of the studied sorbents.

For this purpose, the isotherms were approximated using the Langmuir equation: $C_{sorb} = Q_{max} \times K_{La} \times C_{sol}/(1 + K_{La} \times C_{sol})$, where C_{sorb} is the equilibrium concentration of sorbed radionuclides, C_{sol} is the equilibrium concentration of radionuclides in aqueous solution,

Q_{max} is the maximum sorption capacity, and K_{La} is the sorption coefficient. The data on maximal U(VI) sorption capacity summarized in Table 1 demonstrate even more evident trend. The other fitting parameters and parameters for fitting sorption isotherms using the Freundlich equation are presented in Table S1. The sorption capacity of AG is doubled already after a relatively short oxidation treatment (from 644 to 1210 μmol/g after 6 h treatment). The longer is the oxidation treatment, the higher is the oxidation degree (smaller C/O ratio) and the stronger is the increase in sorption capacity (Table 1). An enormously high sorption capacity of 5400 μmol/g was found for SOAG material subjected to the longest oxidation treatment and having the highest oxidation degree (C/O=2.35). It is interesting to note that the highest sorption is observed for the samples with the maximal degree of oxidation despite lower specific surface area (Fig. 6 a, b) and total pore volume.

The total sorption of U(VI) by SOAG materials is among the highest values ever reported for carbon materials (Table 3). Table 3 shows some representative data for U(VI) sorption by graphene-related materials and different other types of carbons. It is interesting to note a large scatter in the sorption values reported for pristine graphene oxide. Our earlier studies [6,15] demonstrated about 10-fold smaller sorption compared to some other reports. [14] The difference could be at least partly related to different defect state of studied graphene oxides, as it was demonstrated in our earlier study of the defect-rich dGO material.[16] In the latter case the increase in sorption by about 20 times up to 2250 μmol/g was related to intentionally introduced defects [16]. The SOAG materials with the highest degree of oxidation showed about twice higher sorption of U(VI) compared to dGO and possibly the highest sorption compared to all other carbon materials reported so far.

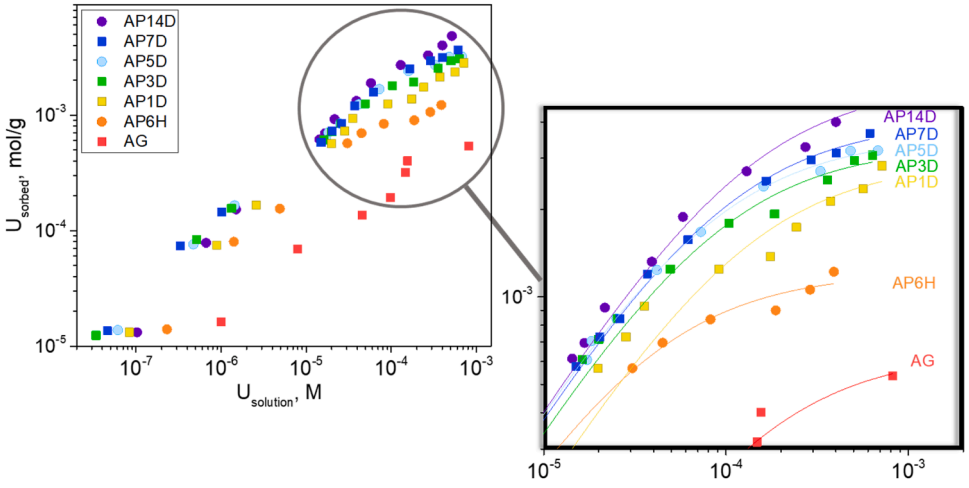

Fig. 5. Isotherms of U(VI) sorption. U(VI) sorption onto SOAG samples with progressively longer oxidation treatment (6 h to 14 days) and different oxidation degrees. Inset shows zoomed part of isotherms.

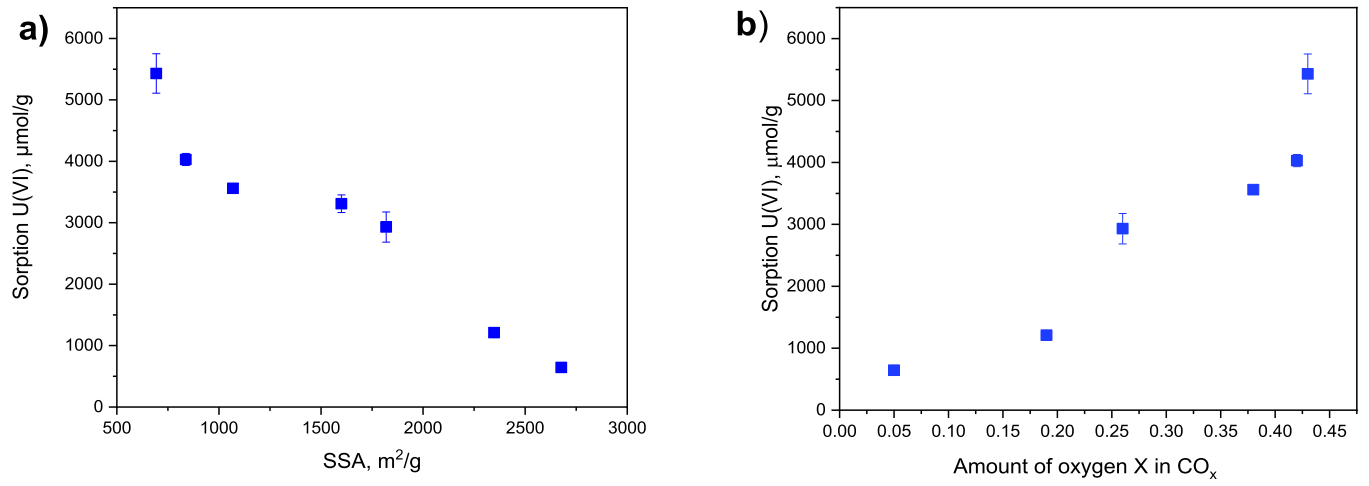

Fig. 6. Trends in sorption of U(VI) by SOAG materials. Sorption of U(VI): a) versus SSA value and b) versus oxidation degree X in the formula COx calculated using C/O ratio provided by XPS analysis.

Our experiments allow to evaluate general trends in U(VI) sorption in relation to specific surface area, pore size distribution and oxidation degree of the SOAG material. These trends can be used in future to design new materials with even higher sorption of U(VI) and other radionuclides.

3.3. Mechanism of sorption and general trends in sorption of U(VI) by oxidized graphene-related materials

Porous carbon materials exhibit very high specific surface areas but they are not efficient in U(VI) sorption due to the absence of suitable binding sites. Surface oxidation studied here using example of AG results in the extensive functionalization of carbon surface with variety of oxygen-containing groups. Because of rather irregular and completely disordered porous structure of AG the oxygen groups are attached to carbon surface in random positions and orientations. Moreover, several types of oxygen functional groups are found in SOAG according by XPS and FTIR (Figs. 3,4). Therefore, the detailed analysis of sorption mechanism in SOAG e.g. using electron spectroscopy methods and theoretical modeling is rather difficult. Any method will provide the data averaged over many possible sorption sites of SOAG and many types of functional groups revealed by the XPS and FTIR.

The detailed characterization and modelling of sorption mechanism was reported in our earlier study for the SOAG sample with C/O= 3.3, BET SSA of 880 m^2/g and total sorption of 1950 µmol/g [20]. The sample was studied after U(VI) sorption using combination of EXAFS and HERFD-XANES spectroscopies. The analysis of spectra and theoretical modelling indicated that the experimental data are compatible with U(VI) adsorbed in small holes rather abundant in extremely defect-rich AG surface and related to carboxylic oxygen functional groups terminating the edges of these holes. The mechanism of U(VI) sorption by SOAG materials was also found to be similar to the sorption by defect-rich graphene oxides.[16] In fact, the SOAG can even be named as “3D graphene oxide” considering its similarity in many properties to dGO.[20] More detailed analysis of the similarities and differences in U(VI) sorption by graphene oxides and SOAG taking into account the whole set of super-oxidized samples is provided below.

According to XPS and FTIR data, the degree of oxidation achieved in the SOAG materials after 5–10 days of treatment is rather similar to graphene oxides extensively studied in previous years for sorption of radionuclides[15,16]. Typical GO synthesized by the Hummers method (HGO) showed an oxidation degree higher than that of AP14D but a lot smaller sorption. The maximal U(VI) sorption capacity of standard HGO was evaluated in our earlier study to be about 120 µmol/g for material with C/O= 2.2. The sorption capacity of GO increased only when a large number of hole defects had been introduced via a specially designed synthesis procedure. The defect rich graphene oxide (dGO) showed a very strong increase in the U(VI) sorption capacity up to 2250 µmol/g for the sample with lower oxidation degree (C/O= 2.7) [16]. However, very large maximal sorption capacity in dGO is still twice lower than that of the AP14D sample.

The difference between sorption properties of GO, dGO and SOAG materials demonstrates that not only the degree of oxidation but also the nature of the oxygen species is an important parameter affecting overall sorption capacity. The larger part of oxygen in the standard GO is not contributing to U(VI) sorption, as it is evidenced by a very low sorption of nearly defect-free Brodie GO.[15] These oxygen species are hydroxyls and epoxy groups attached to the planar surface of GO sheets. The modeling of U(VI) sorption mechanism showed that carboxylic groups attached to the edges of small holes are the main binding sites in GO and dGO.[15] However, the number of hole defects in graphene oxide sheets cannot be increased too much, unless 2D sheets are split into small fragments. (Fig. 7).

In contrast, the strongly oxidized surface of the porous carbon material can be imagined as “graphene oxide” with extreme number of defects, not achievable in true GO, but with somewhat similar type of oxidation as evidenced by FTIR, XPS and TGA data shown above. As it is shown in Table 2 and 3, the overall oxidation degree of the SOAG material also correlates with the relative amount of carboxyl/carbonyl groups which can be used as a measure of defectiveness of the carbon material. The mechanism of sorption related to high abundance of defects and carboxylic groups terminating the defects in SOAG materials is also confirmed by the XPS spectra of two samples after sorption of U(VI) (Fig. 8). Indeed, higher uranium content in AP14D than in AP6H as revealed by the larger area of U4f peak in the spectrum of the former sample (Fig. 8b) well correlates with the higher intensity of the O= C−O component in the C1s spectrum of AP14D (Fig. 8a). At the same time the intensities of the C−O components are about the same in both C1s spectra. The U4f spectra (Fig. 8b) show well pronounced satellites separated from the main peaks for about 3.2 eV, which is typical for U^{6+}, but slightly lower than in UO_3 oxide.[37] Smaller separation between satellites and main peaks in the studied samples (3.2 eV) than in the bulk uranium compounds (3.6–4.2 eV) [37] indirectly confirms the adsorbed nature on the U^{6+} species in the samples.

Oxidized AG is a microporous material with the narrow pore size distribution limited to diameter below 1 nm. The inner surface of these pores must be covered with oxygen functional groups according to the high abundance of oxygen detected by XPS. Therefore, instead of small holes accommodating U(VI) in defects of graphene oxide sheets, SOAG material provide the whole pore length for uranyl ion sorption. Notably,

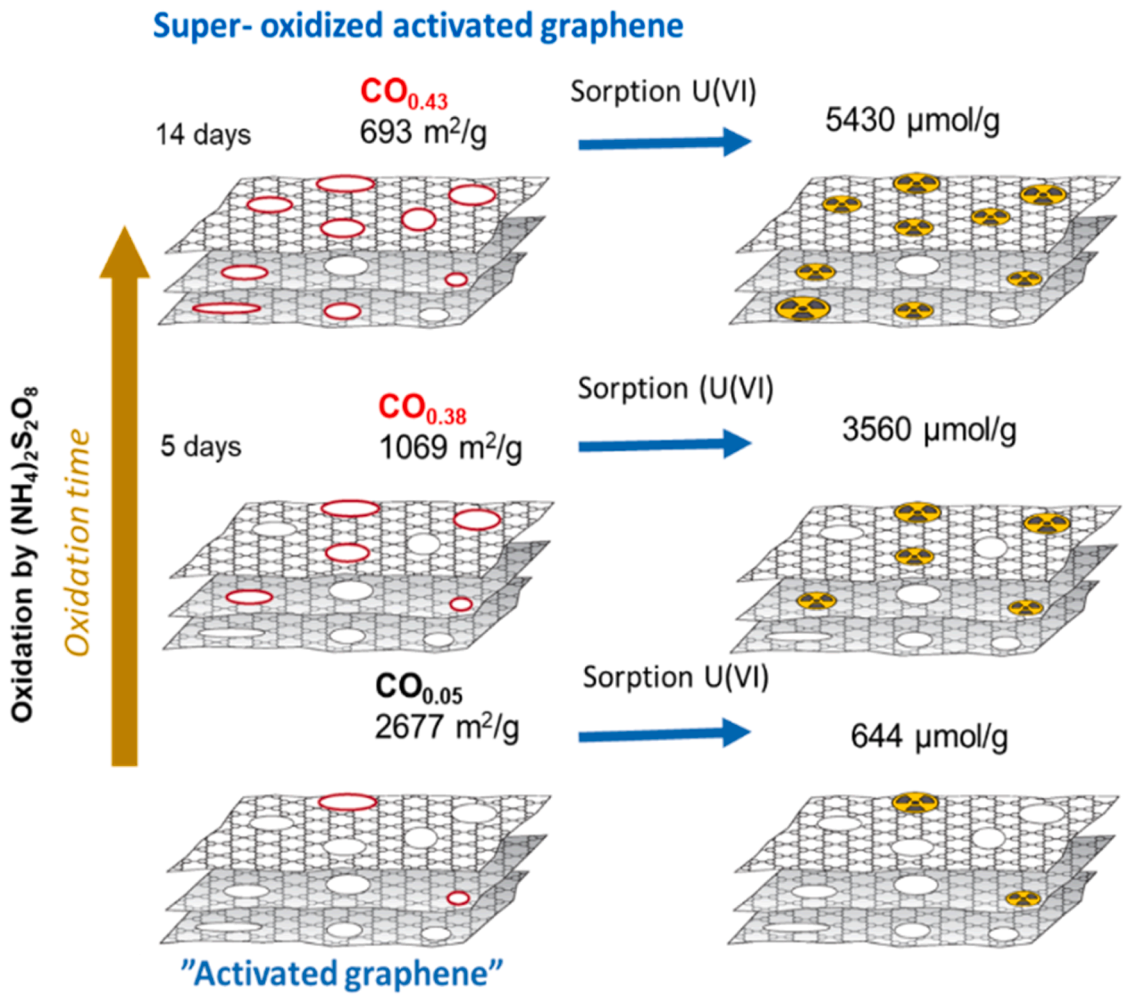

Fig. 7. The scheme illustrating correlations between oxidation degree, surface surface area and sorption of U(VI).

Table 3
U(VI) sorption capacities of carbon materials studied in this work and reported in literature.

Sorbent	pH value	U (VI) sorption capacity, µmol/g	Reference
Graphene-related materials			
Graphene oxides	5	116	[6,15] (by authors of this study)
Graphene oxide	4	1256	[14]
Graphene oxide-activated carbon felt	5.5	1252	[28]
GO@chitosan	6	2117	[29]
Defect-rich graphene oxide (dGO)	5.1	2250 ± 50	[16] (by authors of this study)
SOAG	5.1	1950 ± 60	[20] (by authors of this study)
SOAG" (C/O =2.3)	5,1	**5400 ± 300**	**This work**
Other carbon materials			
Biochar	5.5	114	[30]
Activated carbon	3	119	[31]
Carbon nanotubes	5	166	[32]
Modified carbon nanotubes	5	193	[33]
(CMPEI)-modified mesoporous carbon	4	1050	[34]
Cross-linked chitosan	4	2029	[35]
Spent coffee grounds	3	2770	[36]

the size of uranyl ion in hydrated state is about 5 Å [38] which is close to the pore size of strongly oxidized AG (8–9 Å). Remarkably, the collapse of mesopores (2–4 nm) in oxidized AG seem not to affect the sorption properties of these materials. Micropores in the SOAG materials are sufficiently large for penetration of uranyl ions.

Moreover, the specific surface area of graphene oxide measured in dispersions by ion sorption is only ~600–800 m^2/g, much below than theoretical specific surface area of graphene oxide (~2200 m^2/g) [39]. Graphene oxide is a true 2D material when it is well dispersed in water (most commonly by sonication) but even in dispersions it tend to aggregate into 3–4 layered flakes. The BET surface area of dry powder GO is close to zero due to restacking of individual sheets into multi-layered structures. The interlayer distance in multilayered GO is too small for penetration of nitrogen molecules resulting in the negligible BET surface area. In contrast, the best porous carbons exhibit much higher BET surface area exceeding 3000 m^2/g. This surface area is accessible for oxidation without need for dispersing the material. The three-dimensional porous high surface area structure of the precursor preserves even after strong oxidation when some pores collapse. The surface area of SOAG materials is available for sorption of ions directly after immersion of powder into solutions. In contrast, both standard GO and dGO require sonication for dispersing 2D sheets and relatively strong centrifuging for separation of the sorbent from the solution. The advantage of SOAG materials is a stable 3D structure and fixed pore size both inside and outside the solution. A simple removal of contaminants can be performed for example using powder material inside of the net bag soaked into solution and removed after sorption is completed.

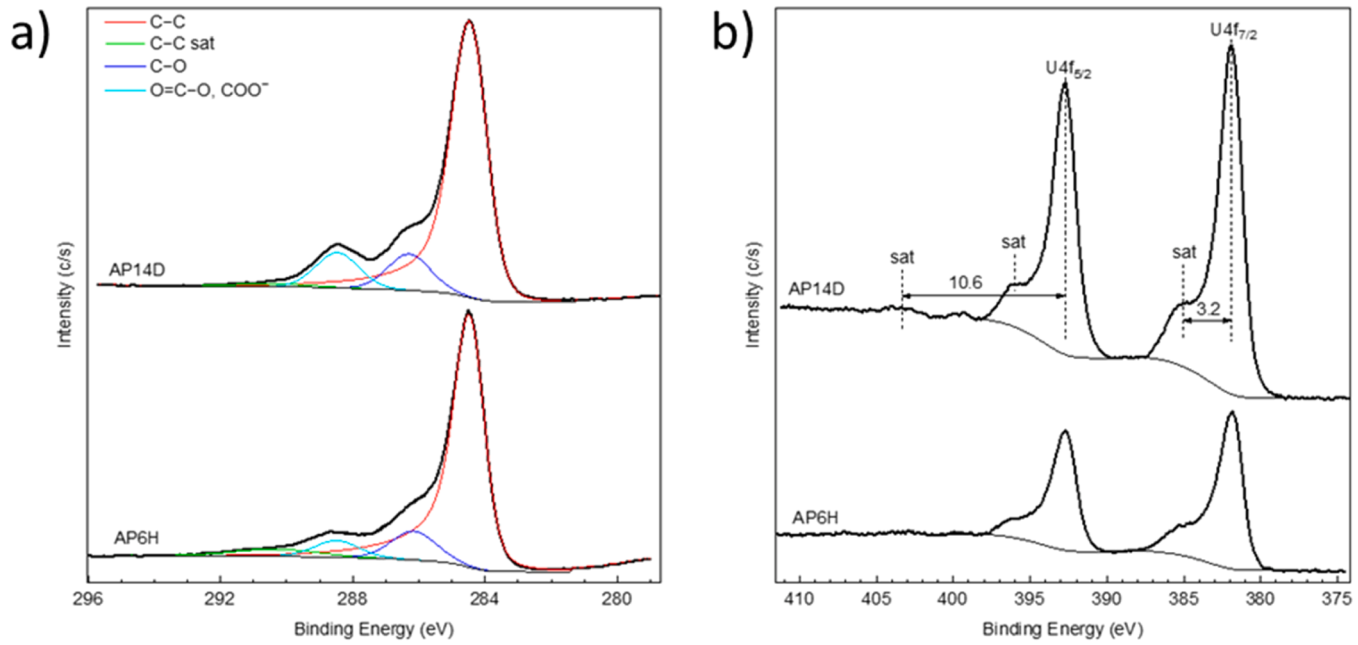

Fig. 8. High-resolution XPS spectra of SOAG samples after sorption of U(VI): a) C1s spectra and b) U4f spectra.

Moreover, we believe that the maximal sorption of SOAG can be further improved using trends presented in our study (see Fig. 6a, b). It is obvious that the sorption increases with increasing the oxidation degree despite a strong drop in the surface area of the samples. However, the specific surface area and oxidation degree are not completely independent parameters in our experiments. The ideal dataset would include sorption data for the materials with exactly the same specific surface area but different degree of oxidation. However, the oxidation methods used in our experiments result in unavoidable sacrifice of surface area. The plots in Fig. 6 reflect the fact that the surface oxidation resulted in partial collapse of pore structure and decrease in surface area. However, the overall number of oxygen groups available as sorption sites becomes larger in more strongly oxidized sample as it is evident from the sorption results. It can be assumed that nearly all oxygen-containing functional groups are located at the surface of material and accessible for sorption of U(VI). The overall amount of oxygen groups per unit of area increases in the samples subjected to prolonged oxidation stronger than the drop in total surface area. Assuming the graphene-like surface for the simplest estimation (~38 carbon atoms per nm^2) the density of oxygen –containing functional groups in the sample with the strongest oxidation (AP14D) is about 16 per nm^2 if calculated considering $CO_{0.43}$ composition.

Therefore, it can be predicted that hypothetical material with the oxidation degree similar to the AP14D sample (C/O=2.30, $CO_{0.43}$) and specific surface area of precursor AG (~2700 m^2/g) could provide the total sorption for U(VI) of about 3.7 times higher, that is ~20 000 μmol/g.

This extremely high sorption value can be achieved only assuming idealized material, which has complete surface oxidation without any collapse of pores. The value of ~20 000 μmol/g is only a hypothetical highest limit number unlikely to be achieved in real material. However, further increase in the U(VI) sorption could possibly be achieved for precursor materials with even higher specific surface area (>3000 m^2/g) and using some hypothetical softer and less destructive oxidation methods. It can be noted that experimentally observed sorption of U(VI) reported in our study (~5400 μmol/g) is already exceptionally high.

The exceptionally high sorption capacity of SOAG materials could be useful in removal of radioactive and heavy metals contaminations e.g. from strongly contaminated industrial waste solutions, mining waste or from water contaminated in nuclear plan accidents (e.g. Fukushima-kind of accidents). Moreover, using other porous carbons as inexpensive replacements of AG such as high surface area activated carbons, could provide a way to design of new sorbent materials for practical industrial scale applications. In fact, AG produced by KOH activation of rGO is very similar to high surface area activated carbons.[40] However, one need to note that the ability of various porous carbons to maintain high surface area under conditions of strong oxidation might be significantly different as evidenced by the test experiment with activated carbon demonstrating lower stability of this material against oxidation-induced collapse of porous structure.

4. Conclusions

In conclusion, a single batch of “activated graphene” with the specific surface area of about 2700 m^2/g was split into smaller samples and oxidized for different times by ammonium persulfate. The surface of the oxidized samples showed an oxidation degree up to C/O~2.4 and a type of surface functionalization with oxygen groups similar to strongly defected graphene oxide. The strong surface oxidation resulted in the decrease in the specific surface area due to collapse of mesopores with only smallest sub-nanometer pores preserving after treatment. The SOAG samples were tested in the sorption of U(VI), which revealed a clear correlation of the sorption capacity with the overall oxidation degree of the SOAG material despite the decrease in the specific surface area and pore volume caused by partial oxidation-induced collapse of porous structure. An exceptionally high sorption of U(VI) of about 5400 μmol/g was achieved in the solution with pH 5.1 for the sample with the highest oxidation degree (C/O=2.35) and SSA of 693 m^2/g. This sample demonstrated 8.4-fold increase in the maximal U(VI) sorption compared to non-oxidized precursor AG. The maximal sorption of U(VI) by the best SOAG sample is also ~50 times higher than that of standard GO and about 2 times higher than that of defect-rich GO [16]. The enormous sorption of U(VI) is related to rather high density of oxygen functional groups per unit of area in SOAG materials. Therefore, further increase in sorption capacity is likely to be achieved using softer oxidation methods capable to preserve most of the surface area of the precursor material while providing similarly high degree of oxidation. It is also very likely that other types of porous carbons can be oxidized using proposed method to the similarly high degree thus opening a road to new class of surface oxidized high surface area porous carbons.

Environmental implication

Developing new sorbents to remove radionuclide contaminations from the environment is important and challenging task. Uranium is hazardous in many ways and its presence in the environment can have harmful effects on animals and humans. The development of effective sorbents can help to reduce the levels of uranium in contaminated soil and water, potentially improving the health of local ecosystems and human populations. The sorbents which we designed are extremely efficient in removing U(VI) demonstrating record high capacity compared to other state of art materials. These sorbents can be used for cleaning industrial waste waters using standard filtration devices.

CRediT authorship contribution statement

Alexandr V. Talyzin: Conceptualization, Investigation, Methodology, Supervision, Writing- Original draft preparation. **Stepan N. Kalmykov**: Conceptualization, Supervision, writing-editing. **Anna Yu. Romanchuk:** Conceptualization, Investigation, Methodology, Writing-Original draft preparation. **Konstantin I. Maslakov:** Data Curation. **Tamuna Bakhiia:** Data Curation, Investigation **Gui Li:** Data Curation. **Nicolas Boulanger:** Data Curation, Investigation, Figure preparations. All authors participated in discussion of results and preparation of final version of manuscript.

Declaration of Competing Interest

The authors declare that they have no known competing financial interests or personal relationships that could have appeared to influence the work reported in this paper.

Data Availability

Data will be made available on request.

Acknowledgements

AT acknowledge the Vibrational Spectroscopy Platform as well as the Umeå Core Facility Electron Microscopy (UCEM) of Umeå University and A. Shchukarev for support with the XPS characterization. The authors acknowledge support from the Lomonosov Moscow State University Program of Development. A.T. also acknowledges European Union's Horizon 2020 research and the innovation program under grant agreement no. 881603 (ATN). B., AYR., SNK acknowledge support by the Russian Ministry of Science and Education under Grant no. 075-15-2021- 1353.

Conflicts of interest

The authors declare no financial or commercial conflict of interest.

Appendix A. Supporting information

Supplementary data associated with this article can be found in the online version at doi:10.1016/j.jhazmat.2023.131817.

References

[1] Aylmore, L.A.G., Quirk, J.P., 1959. Swelling of clay-water systems. Nature 183, 1752–1753.
[2] Lerf, A., Buchsteiner, A., Pieper, J., Schottl, S., Dekany, I., Szabo, T., et al., 2006. Hydration behavior and dynamics of water molecules in graphite oxide. J Phys Chem Solids 67, 1106–1110.
[3] Szabo, T., Berkesi, O., Forgo, P., Josepovits, K., Sanakis, Y., Petridis, D., et al., 2006. Evolution of surface functional groups in a series of progressively oxidized graphite oxides. Chem Mater 18, 2740–2749.
[4] Szabo, T., Tombacz, E., Illes, E., Dekany, I., 2006. Enhanced acidity and pH-dependent surface charge characterization of successively oxidized graphite oxides. Carbon 44, 537–545.
[5] Iakunkov, A., Talyzin, A.V., 2020. Swelling properties of graphite oxides and graphene oxide multilayered materials. Nanoscale 12, 21060–21093.
[6] Romanchuk, A.Y., Slesarev, A.S., Kalmykov, S.N., Kosynkin, D.V., Tour, J.M., 2013. Graphene oxide for effective radionuclide removal. Phys Chem Chem Phys 15, 2321–2327.
[7] Milford, M.H., Jackson, M.L., 1962. Specific surface determination of expansible layer silicates. Science 135, 929-&.
[8] Otowa, T., Nojima, Y., Miyazaki, T., 1997. Development of KOH activated high surface area carbon and its application to drinking water purification. Carbon 35, 1315–1319.
[9] Klechikov, A., Mercier, G., Sharifi, T., Baburin, I.A., Seifert, G., Talyzin, A.V., 2015. Hydrogen storage in high surface area graphene scaffolds. Chem Commun 51, 15280–15283.
[10] Iakunkov, A., Skrypnychuk, V., Nordenstrom, A., Shilayeva, E.A., Korobov, M., Prodana, M., et al., 2019. Activated graphene as a material for supercapacitor electrodes: effects of surface area, pore size distribution and hydrophilicity. Phys Chem Chem Phys 21, 17901–17912.
[11] Zhu, Y.W., Murali, S., Stoller, M.D., Ganesh, K.J., Cai, W.W., Ferreira, P.J., et al., 2011. Carbon-based supercapacitors produced by activation of graphene. Science 332, 1537–1541.
[12] H.P. Boehm, A. Clauss, G. Fischer, C. Hofmann, Surface Properties of Extremely Thin Graphite Lamellae, Proc. 5th Conf. on Carbon (Oxford: Pergamon) (1962) 73–80.
[13] Montes-Navajas, P., Asenjo, N.G., Santamaria, R., Menendez, R., Corma, A., Garcia, H., 2013. Surface area measurement of graphene oxide in aqueous solutions. Langmuir 29, 13443–13448.
[14] Li, Z.J., Chen, F., Yuan, L.Y., Liu, Y.L., Zhao, Y.L., Chai, Z.F., et al., 2012. Uranium (VI) adsorption on graphene oxide nanosheets from aqueous solutions. Chem Eng J 210, 539–546.
[15] Kuzenkova, A.S., Romanchuk, A.Y., Trigub, A.L., Maslakov, K.I., Egorov, A.V., Amidani, L., et al., 2020. New insights into the mechanism of graphene oxide and radionuclide interaction. Carbon 158, 291–302.
[16] Boulanger, N., Kuzenkova, A.S., Iakunkov, A., Romanchuk, A.Y., Trigub, A.L., Egorov, A.V., et al., 2020. Enhanced sorption of radionuclides by defect-rich graphene oxide. Acs Appl Mater Inter 12, 45122–45135.
[17] Datsyuk, V., Kalyva, M., Papagelis, K., Parthenios, J., Tasis, D., Siokou, A., et al., 2008. Chemical oxidation of multiwalled carbon nanotubes. Carbon 46, 833–840.
[18] Guedidi, H., Reinert, L., Leveque, J.M., Soneda, Y., Bellakhal, N., Duclaux, L., 2013. The effects of the surface oxidation of activated carbon, the solution pH and the temperature on adsorption of ibuprofen. Carbon 54, 432–443.
[19] Khannanov, A., Nekljudov, V.V., Gareev, B., Kiiamov, A., Tour, J.M., Dimiev, A.M., 2017. Oxidatively modified carbon as efficient material for removing radionuclides from water. Carbon 115, 394–401.
[20] Boulanger, N., Kuzenkova, A.S., Iakunkov, A., Nordenstrom, A., Romanchuk, A.Y., Trigub, A.L., et al., 2022. High surface area "3D Graphene Oxide" for enhanced sorption of radionuclides. Adv Mater Interfaces 9.
[21] Amirov, R.R., Shayimova, J., Nasirova, Z., Solodov, A., Dimiev, A.M., 2018. Analysis of competitive binding of several metal cations by graphene oxide reveals the quantity and spatial distribution of carboxyl groups on its surface. Phys Chem Chem Phys 20, 2320–2329.
[22] Amirov, R.R., Shayimova, J., Nasirova, Z., Dimiev, A.M., 2017. Chemistry of graphene oxide. Reactions with TRansition Metal Cations. Carbon 116, 356–365.
[23] Rouquerol, J., Llewellyn, P., Rouquerol, F., 2006. Is the BET equation applicable to microporous adsorbents? Stud Surf Sci Catal 160, 49–56.
[24] Osterrieth, J.W.M., Rampersad, J., Madden, D., Rampal, N., Skoric, L., Connolly, B., et al., 2022. How reproducible are surface areas calculated from the BET equation? Adv Mater 34.
[25] Findenegg, G.H., Jahnert, S., Akcakayiran, D., Schreiber, A., 2008. Freezing and melting of water confined in silica nanopores. Chemphyschem 9, 2651–2659.
[26] Korobov, M.V., Talyzin, A.V., Rebrikova, A.T., Shilayeva, E.A., Avramenko, N.V., Gagarin, A.N., et al., 2016. Sorption of polar organic solvents and water by graphite oxide: Thermodynamic approach. Carbon 102, 297–303.
[27] Lerf, A., He, H.Y., Forster, M., Klinowski, J., 1998. Structure of graphite oxide revisited. J Phys Chem B 102, 4477–4482.
[28] Chen, S.P., Hong, J.X., Yang, H.X., Yang, J.Z., 2013. Adsorption of uranium (VI) from aqueous solution using a novel graphene oxide-activated carbon felt composite. J Environ Radioact 126, 253–258.
[29] Sharma, M., Laddha, H., Yadav, P., Jain, Y., Sachdev, K., Janu, V.C., et al., 2022. Selective removal of uranium from an aqueous solution of mixed radionuclides of uranium, cesium, and strontium via a viable recyclable GO@chitosan based magnetic nanocomposite. Mater Today Commun 32.
[30] Mishra, V., Sureshkumar, M.K., Gupta, N., Kaushik, C.P., 2017. Study on sorption characteristics of uranium onto biochar derived from eucalyptus wood. Water Air Soil Poll 228.
[31] Mellah, A., Chegrouche, S., Barkat, M., 2006. The removal of uranium(VI) from aqueous solutions onto activated carbon: Kinetic and thermodynamic investigations. J Colloid Interface Sci 296, 434–441.
[32] Fasfous, I.I., Dawoud, J.N., 2012. Uranium (VI) sorption by multiwalled carbon nanotubes from aqueous solution. Appl Surf Sci 259, 433–440.
[33] Schierz, A., Zanker, H., 2009. Aqueous suspensions of carbon nanotubes: Surface oxidation, colloidal stability and uranium sorption. Environ Pollut 157, 1088–1094.

[34] Kim, J.H., Lee, H.I., Yeon, J.W., Jung, Y., Kim, J.M., 2010. Removal of uranium(VI) from aqueous solutions by nanoporous carbon and its chelating polymer composite. J Radio Nucl Ch 286, 129–133.
[35] Humelnicu, D., Dinu, M.V., Dragan, E.S., 2011. Adsorption characteristics of UO22 + and Th4+ ions from simulated radioactive solutions onto chitosan/clinoptilolite sorbents. J Hazard Mater 185, 447–455.
[36] Ma, J.H., Zhang, M., Zhang, H., Wang, Y.D., Li, F., Hu, N., et al., 2022. Efficient removal of U(VI) in acidic environment with spent coffee grounds derived hydrogel. J Hazard Mater 426.
[37] Ilton, E.S., Bagus, P.S., 2011. XPS determination of uranium oxidation states. Surf Interface Anal 43, 1549–1560.
[38] Perez-Conesa, S., Torrico, F., Martinez, J.M., Pappalardo, R.R., Marcos, E.S., 2016. A hydrated ion model of [UO2](2+) in water: Structure, dynamics, and spectroscopy from classical molecular dynamics. J Chem Phys 145.
[39] Klechikov, A., Sun, J.H., Hu, G.Z., Zheng, M.B., Wagberg, T., Talyzin, A.V., 2017. Graphene decorated with metal nanoparticles: Hydrogen sorption and related artefacts. Microporous Mesoporous Mater 250, 27–34.
[40] Nordenstrom, A., Boulanger, N., Iakunkov, A., Li, G., Mysyk, R., Bracciale, G., et al., 2022. High-surface-area activated carbon from pine cones for semi-industrial spray deposition of supercapacitor electrodes. Nanoscale Adv 4, 4689–4700.